Journal of Macromolecular Science, Part A
Publication details, including instructions for authors and subscription information:
http://www.informaworld.com/smpp/title~content=t713597274

Synthesis and Liquid Crystalline Behavior of Random Copolymer of Poly(ethylene oxide) Macromonomer and Liquid Crystalline Monomer by the Photon Transmission Technique

Sevtap Yildiz[a]; Faruk Yilmaz[bc]; Haluk Özbek[ad]; Önder Pekcan[e]; Koch Ito[f]; Yusuf Yagc[b]
[a] Department of Physics, Istanbul Technical University, Istanbul, Turkey [b] Department of Chemistry, Istanbul Technical University, Istanbul, Turkey [c] Department of Chemistry, Gebze Institute of Technology, Gebze, Kocaeli, Turkey [d] Feza Gursey Institute, Istanbul, Turkey [e] Department of Physics, Işik University, Istanbul, Turkey [f] Department of Materials Science, Toyohashi University of Technology, Toyohashi, Japan

To cite this Article Yildiz, Sevtap , Yilmaz, Faruk , Özbek, Haluk , Pekcan, Önder , Ito, Koch and Yagc, Yusuf(2005) 'Synthesis and Liquid Crystalline Behavior of Random Copolymer of Poly(ethylene oxide) Macromonomer and Liquid Crystalline Monomer by the Photon Transmission Technique', Journal of Macromolecular Science, Part A, 42: 12, 1573 — 1588
To link to this Article: DOI: 10.1080/10601320500246602
URL: http://dx.doi.org/10.1080/10601320500246602

Journal of Macromolecular Science®, Part A: Pure and Applied Chemistry, 42:1573–1588, 2005

ISSN 1060-1325 print/1520-5738 online
DOI: 10.1080/10601320500246602

Synthesis and Liquid Crystalline Behavior of Random Copolymer of Poly(ethylene oxide) Macromonomer and Liquid Crystalline Monomer by the Photon Transmission Technique

SEVTAP YILDIZ,[1] FARUK YILMAZ,[2,3] HALUK ÖZBEK,[1,4] ÖNDER PEKCAN,[5] KOİCHİ ITO,[6]* AND YUSUF YAGCİ[2]

[1]Istanbul Technical University, Department of Physics, Istanbul, Turkey
[2]Istanbul Technical University, Department of Chemistry, Istanbul, Turkey
[3]Gebze Institute of Technology, Department of Chemistry, Gebze, Kocaeli, Turkey
[4]Feza Gursey Institute, Istanbul, Turkey
[5]Işik University, Department of Physics, Istanbul, Turkey
[6]Department of Materials Science, Toyohashi University of Technology, Tempaku-cho, Toyohashi, Japan

Random copolymers of poly(ethylene oxide) macromonomer with p-vinylbenzyl end-functional group (PEOVB) and liquid crystalline monomer, namely 6-(4-cyanobiphenyl-4′-oxy)hexyl acrylate (COA), were prepared by conventional free radical polymerization. A living anionic polymerization technique was employed for the synthesis of PEO macromonomers bearing p-vinylbenzyl moiety at one end. The photon transmission method was also applied to study the phase transitions of COA monomer and its random copolymer with PEO. It was found that, for both samples, the nematic-smectic A transition is continuous, but the critical fluctuation regions do not allow to obtain 3D XY values. Instead, we have obtained the values close to mean field regime. Scaling of thermal hystersis for random copolymer sample near the nematic-isotropic transition was studied as well. Thermal hysteresis loops were produced under linearly varying temperature. It was shown that the areas of the hysteresis loops scale with the temperature scanning rate with an exponent being equal to 0.614 which is in good agreement with the field-theoretical value.

Keywords PEO macromonomer, liquid crystalline monomer, photon transmission method, nematic and smectic ordering, critical exponent, scaling of thermal hysteresis

Received April 2005; Accepted May 2005.
*Present address: 34-1 Kitazawa, Takashi-hongo, Toyohashi, 441-8153 Japan.
Address correspondence to Sevtap Yıldız, Istanbul Technical University, Department of Physics, Istanbul 34469, Turkey. E-mail: sevtap@itu.edu.tr; Yusuf Yagci, Istanbul Technical University, Department of Chemistry, Istanbul 34469, Turkey. E-mail: yusuf@itu.edu.tr

Introduction

At present, there is a rapid development of research activity on the synthesis, physical properties, and applications of materials in the fields of polymer and material science. One of the existing methods of improving polymer properties is the copolymerization.

Macromonomers are short macromolecular chains that are end-capped with a polymerizable group(s) capable of copolymerizing with a low-molar-mass comonomer to synthesize block and graft copolymers, star polymers, and polymer networks copolymers. Various polymerization techniques including anionic, cationic, radical polymerizations and chemical modifications of polymer ends can be employed in the preparation of macromonomers (1, 2). For example, on choosing an initiator containing a polymerizable group, macromonomers can be derived provided this reactive group is totally inert toward the active species generated by its carrier. Macromonomers can also be obtained by functionalization of growing chains. It is essential that the end-capping reaction does not involve the polymerizable group. Moreover, modifying ω-functional polymers using post-functionalization methodologies can be another synthetic route leading to macromonomers (3–7).

Anionic living polymerization of ethylene oxide (EO) can be conveniently utilized for the synthesis of poly(ethylene oxide) (PEO) macromonomers with quantitatively functionalized terminals (8–10). Then, the resulting macromonomer can be expected to behave as a building block for synthesizing of block and graft copolymers (11). PEO macromonomers constitute an interesting class of amphiphilic (surface active) monomers, which can aggregate into micelles and be polymerized under both the homogeneous and heterogeneous conditions.

The properties of liquid crystals and those of polymers can be combined in polymer liquid crystals (PLC). These hybrid materials possess the same mesophase characteristics of ordinary liquid crystals; in addition they retain many of the useful and versatile properties of polymers. Consequently, PLCs exhibit thermotropic and lyotropic mesophases as displayed by the thermotropic and lyotropic low molar mass liquid crystals. Various architectures of PLC have been developed in the recent past (12–14), especially random and block copolymers of mesogenic monomers. Side-chain liquid crystal polymers (SCLCP) are prepared when the mesogens are incorporated as side chains to the polymer by a flexible bridge. Over the past few decades, a large number of SCLCPs have been synthesized. This could be possible because of the combination of the vast number of mesogenic units available and many different backbone types possible (e.g. siloxanes, acrylates, methacrylates, ethylenes, epoxides). Both nematic and smectic phases have been generated. The SCLCPs exhibiting a reentrant nematic phase have also been generated. A considerable interest is being given to liquid-crystalline side-chain polymers because of their theoretical aspects and their potential applications, namely electro-optic displays using nematic or smectic mesogenic side-chain polymers (15).

In this work, we report the synthesis of the random copolymers of PEO macromonomer possessing *p*-vinyl benzyl end-group and liquid crystalline 6-(4-cyanobiphenyl-4′-oxy)hexyl acrylate (COA) monomer by conventional free radical polymerization. It is well known that structure determination and phase transition identification of the polymer liquid crystals are essentially based on thermal analysis, optical microscopy, and X-ray measurements. In the present paper, we have also investigated the phase transitions of liquid-crystalline COA monomer and its random copolymer with PEO macromonomer (PCOA-*r*-PEOVB) by using *in situ* photon transmission method, which

was previously described (16–18). Very recently, this method was also used to detect thermal phase transitions in κ-carrageenan-water system (19).

Experimental

Materials

Commercial reagents were purified according to usual procedures. Tetrahydrofuran (THF) was refluxed and distilled over sodium wire. α,α′-Azobisisobutyronitrile (AIBN) was recrystallized from methanol. The reagents used for anionic polymerization of ethylene oxide (EO) and its end-capping were purified and dried by the usual procedure using a vacuum line (10–5 mmHg), and sealed in ampoules fitted with breakable seals. Ethylene oxide (EO) from Seitetsu Chemical Co., Ltd., was distilled twice over potassium hydroxide under argon and twice under vacuum over calcium hydroxide and finally stirred over a sodium mirror for 1 h at 0°C and distilled into a tube with breakable seal. *p*-Vinylbenzyl alcohol was prepared from p-vinylbenzyl chloride (Seimi Chemical Co., Japan) by reaction with sodium acetate followed by alkaline hydrolysis, according to the cited procedure (20).

Synthesis of Liquid Crystalline Monomer, COA

6-(4-Cyanobiphenyl-4′-oxy) hexyl acrylate (COA) were synthesized according to the literature procedure (21). M.p. = 69–71°C, yield: 71%.

^{1}H NMR ($CDCl_3$): δ (ppm) = 1.9–2.0 (m, 8H, $-(CH_2)_4$), 3.9–4.1 (t, 2H, $-OCH_2$), 4.1–4.3 (t, 2H, ArO-CH_2), 5.8–5.9 (d, 1H, $=CH_2$), 6.0–6.2 (m, 1H, =CH), 6.3–6.5 (d, 1H, $=CH_2$), 6.9–7.0 (d, 2H, 3′ and 5′ aromatic protons), 7.5–7.6 (d, 2H, 3 and 5 aromatic protons), 7.6–7.8 (q, 4H, 2, 6 and 2′,6′ aromatic protons).

Synthesis of Poly(etheylene oxide) Macromonomer, PEOVB

The macromonomer was prepared by polymerization of ethyleneoxide with *p*-vinylbenzyl alcohol partially alkoxidated with potassium naphthalene in THF as described in detail (20). The number-average polymerization degree of the PEO chains was determined by ^{1}H NMR measurement by taking the intensity ratio of ethylene oxide peak (*ca* 3.7 ppm) to benzylmethylene (*ca* 4.5 ppm) (Figure 1a).

Synthesis of Random Copolymers

Random copolymers of COA and PEOVB were prepared by free radical polymerization. COA and PEOVB (based on the molecular weight calculated from ^{1}H NMR spectrum in Figure 1a as 1390) were weighed into a glass tube, together AIBN as the initiator and THF as the solvent, and degassed. The tube was then sealed and placed in an oil bath at 60°C for 24 h. The feed molar ratio of COA to PEOVB was taken to be sufficiently large to satisfy simplified treatment of copolymerization. After the reaction time, the copolymer was precipitated and isolated from methanol (stable emulsion resulted), followed by centrifuging and then the recovered product was dried *in vacuo*.

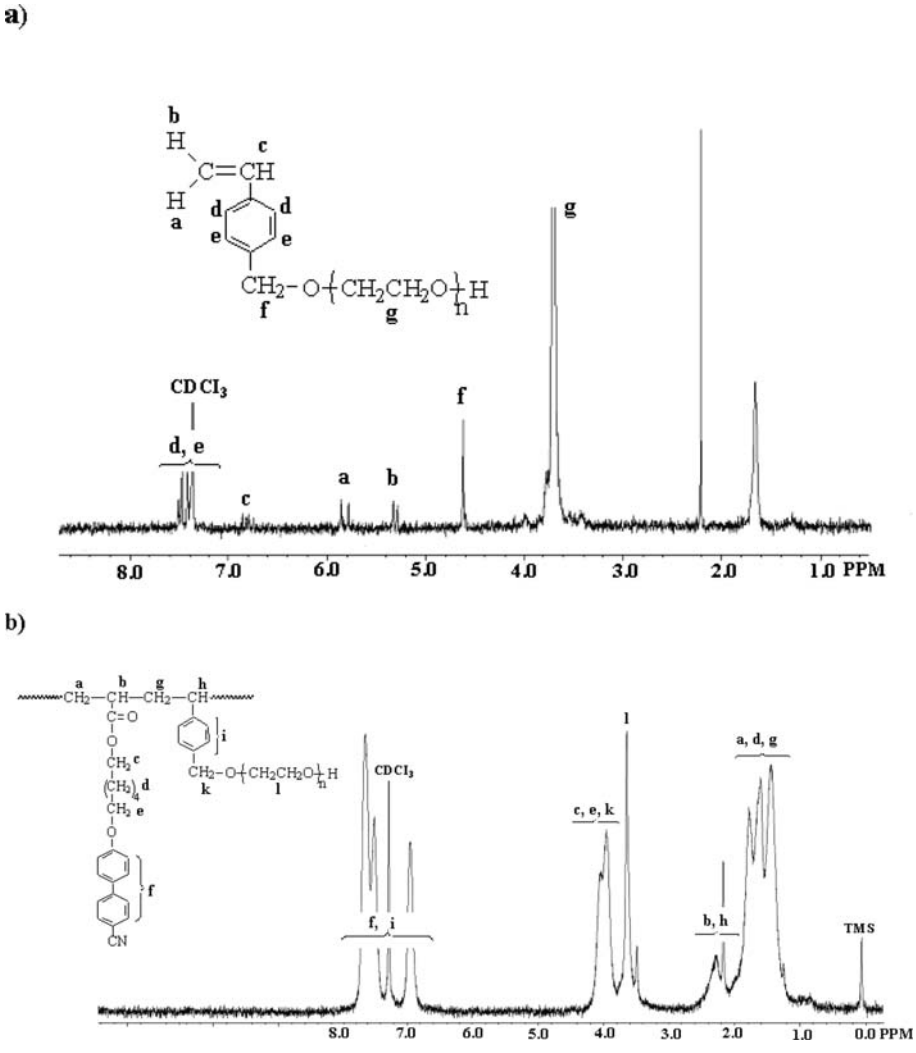

Figure 1. The ^{1}H NMR spectra of PEOVB macromonomer (**a**) and the random copolymer (PCOA-*r*-PEOVB) x = 0.974 (**b**) in $CDCl_3$.

Characterization

^{1}H NMR spectra were measured on a Bruker Am 250 instrument using $CDCl_3$ as the solvent and TMS as the internal standard. Molecular weights and molecular weight distributions were determined using a size exclusion chromatograph consisting of a Waters 600 pump and two ultrastyragel columns (10^4, 500 Å) with THF as the eluent at a flow rate of $1\,mL \cdot min^{-1}$ and a Waters 410 differential refractometer. Molecular weights were calculated with the aid of polystyrene standards.

In situ Measurements

The liquid-crystalline monomer COA and the random copolymer were used without additional purification after having been synthesized. The samples were prepared for

optical measurements separately by placing them into sandwich-cell type glass plane capillary. The thickness of the sample placed between the reference surfaces was determined with a Mylar film of 20 μm thickness. The reference surfaces of sandwich-cell samples were cleaned carefully by using alcohol and acetone (Merck), then they were washed by deionized and bi-distilled water in an ultrasonic bath. Filling of the sandwich-cell with the samples was carried out by capillary action. This was done at temperatures above the isotropization point in order to avoid flow alignment of the director. The planar alignment was obtained by following the procedure, which has previously been described (22).

In-situ photon transmission measurements were performed in real time at 850 nm wavelength using a Jasco V-530 UV/Vis spectrophotometer in time-course mode. The samples under investigation were separately placed within the spectrophotometer and a background count was carried out before *in situ* measurements. The temperature was measured by using an ETC-505T Peltier temperature controller unit equipped with an ETC-505S Peltier thermostatted cell holder and with a Poly Science 8001 programmable circulator. The linear dependence of temperature on time was confirmed by the calibration curve performed by DMA-509 DNA Melting Analysis software package. The block diagram of the experimental setup was given in Reference (23). The structure of the mesophases was identified by a Olympus BHSP polarizing microscope in conjuction with a hot stage, which was designed and produced at the Physics Department, and with a EMKO ESM9320 digital temperature controller. Photon transmission measurements were made on the samples including several heating and cooling runs for each of them, which gave on excellent reproducibility.

Results and Discussion

Synthesis

Macromonomer. The living anionic polymerization of EO with a partially K-alkoxidated functional alcohol has been already established (10, 20, 24). A key point is to avoid any reaction of $KC_{10}H_8$ or the active chain end, K-alkoxide, on the functional group fragment of the initiator during alkoxidation and propagation (Scheme 1). In fact, in the course of the preparation of styrene macromonomer, the attack of $KC_{10}H_8$ on styryl group was essentially avoided by very slow (drop-by-drop) addition of the THF solution into a *p*-vinylphenylalkanol in THF under vigorous magnetic stirring to afford the expected K-alkoxide (2). Then the propagation proceeds normally by ring-opening of EO, since the oxy anion as the propagating species is not reactive enough toward a styryl end-group as an initiator fragment. The degree of polymerization of EO can thus simply be designed by the molar ratio of the EO to the initiator (vinyl benzyl alcohol) in feed, and the molecular weight distribution is sufficiently narrow, with M_w/M_n around 1.05 (Table 1). The molecular weight estimated from the integration of oxyethylene protons to aromatic protons (M_n^{NMR}) is in fairly good agreement with the value expected from the feed ratio ($M_n$theo) and also with that determined by GPC (M_nGPC).

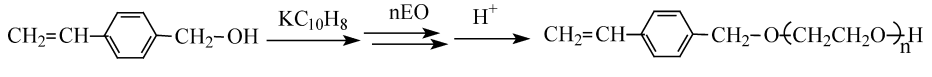

Scheme 1. Synthesis of the macromonomer.

Table 1
The molecular weight characteristics of the macromonomer

$M_n$theo.	M_nNMR	M_nGPC	M_w/M_n	DPnNMR
1370	1390	1470	1.05	28

Random Copolymers. The random copolymer was synthesized via radical polymerization of appropriate COA/PEOVB mixture of different chemical composition in the presence of AIBN as an initiator (Scheme 2). The results of the copolymerization are summarized in Table 2. The structure of the random copolymer was characterized by means of ^{1}H NMR spectroscopy (Figure 1b). The signals at around 6.9–7.6 ppm are assigned to the protons of the phenyl rings. The mole fraction of COA, x, was calculated from the peak area of phenyl protons relative to that of other appropriate protons as follows:

$$\frac{\text{Area of phenyl protons (}\mathbf{f}, \mathbf{i}\text{) at 6.9–7.6}}{\text{Area of protons (}\mathbf{c}, \mathbf{e}, \mathbf{k}, \mathbf{l}\text{) at 3.4–3.9}} = \frac{8x + 4(1 - x)}{4x + (4\bar{n} + 2)(1 - x)}$$

$$\bar{n} = 28 \text{ (Degree of polymerization)}$$

Gel permeation chromatography (GPC) analysis revealed that the PEOVB macromonomer was converted into random copolymers. Curve **a** in Figure 2 shows PEOVB macromonomer. Apparently, this peak is shifted to higher molecular weight (curve **b**) indicating successful random copolymerization of COA.

In-situ Measurements Results

Figures 3(a)–(d) display the transmitted light intensity I_{tr} vs. temperature T data for the liquid-crystalline monomer COA and its random copolymer with PEO (PCOA-*r*-PEOVB) near the nematic-isotropic (N-I) and the nematic-smectic A (N-Sm A) transition regions separately. The temperature dependence of the transmitted intensity suggests that in the temperature range in which I_{tr} changes abruptly a phase transition is detected, which is also confirmed by texture changes in polarization microscopy. Intensity measurements were repeated at several temperature ranges to assure that no measurable changes in the

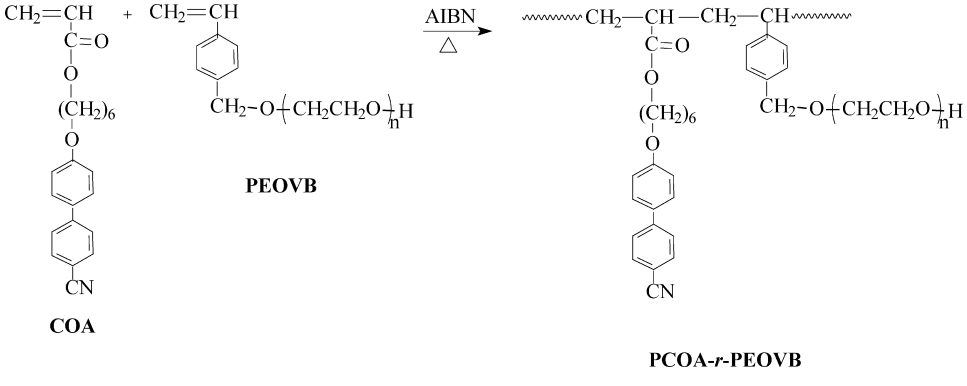

Scheme 2. Synthesis of random copolymers of COA and PEOVB.

Table 2
Preparation of random copolymers of COA and PEOVB. [AIBN] = 2.8×10^{-3} mol L^{-1}; Temp. = 60°C; time = 24 h

Code	[COA] (mol L^{-1})	[COA]/[PEOVB] (mol/mol)	Copoly. Comp. COA (mol %)[a]	M_n[a] (g mol^{-1})	M_w/M_n[b]
PCOA-*r*-PEOVB	0.29	36	97.4	14.400	1.46

[a]Determined by ^{1}H NMR.
[b]Determined by GPC with polystyrene standards.

transmitted intensity had occurred. The phase transition temperatures were determined from the peak positions of the first derivative of the I_{tr} vs. T curves (not shown). It is well known that the sample density has a discontinuity at the nematic-isotropic (N-I) transition, the value in the nematic phase being larger than that in the isotropic phase (25) so a closer packing of the molecules in the nematic phase can be responsible for the lower values observed in this phase and the transmitted intensity I_{tr} decreases as the system goes into the ordered phases. Thus, I_{tr} vs. T data can be somehow related to the temperature dependence of ordering behavior in liquid-crystalline phases. As seen in Figure 3(a–c), the transmitted intensity I_{tr} exhibits discontinious changes at the N-I transitions for both samples.

Thermal hysteresis in the transition temperatures upon heating and cooling was observed at the N-I transition as well. It should be concluded that the N-I transition for both samples (COA and PCOA-r-PEOVB) exhibits first-order transition characteristics, which needs nucleation to occur. These first order N-I transitions of both samples are consistent with the Landau theory of de Gennes (26). For these samples, the phases on each side of the transition were identified by observation of textures between crossed polarizers via polarizing microscope.

The nematic-smectic A (N-Sm A) transition has been the most extensively studied liquid crystalline phase transition both experimentally and theoretically. Considerable

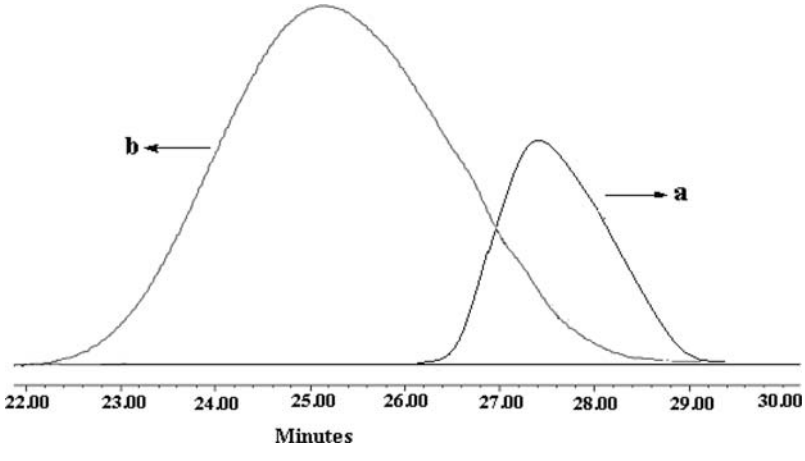

Figure 2. GPC curves of PEOVB (**a**) and the random copolymer (**b**).

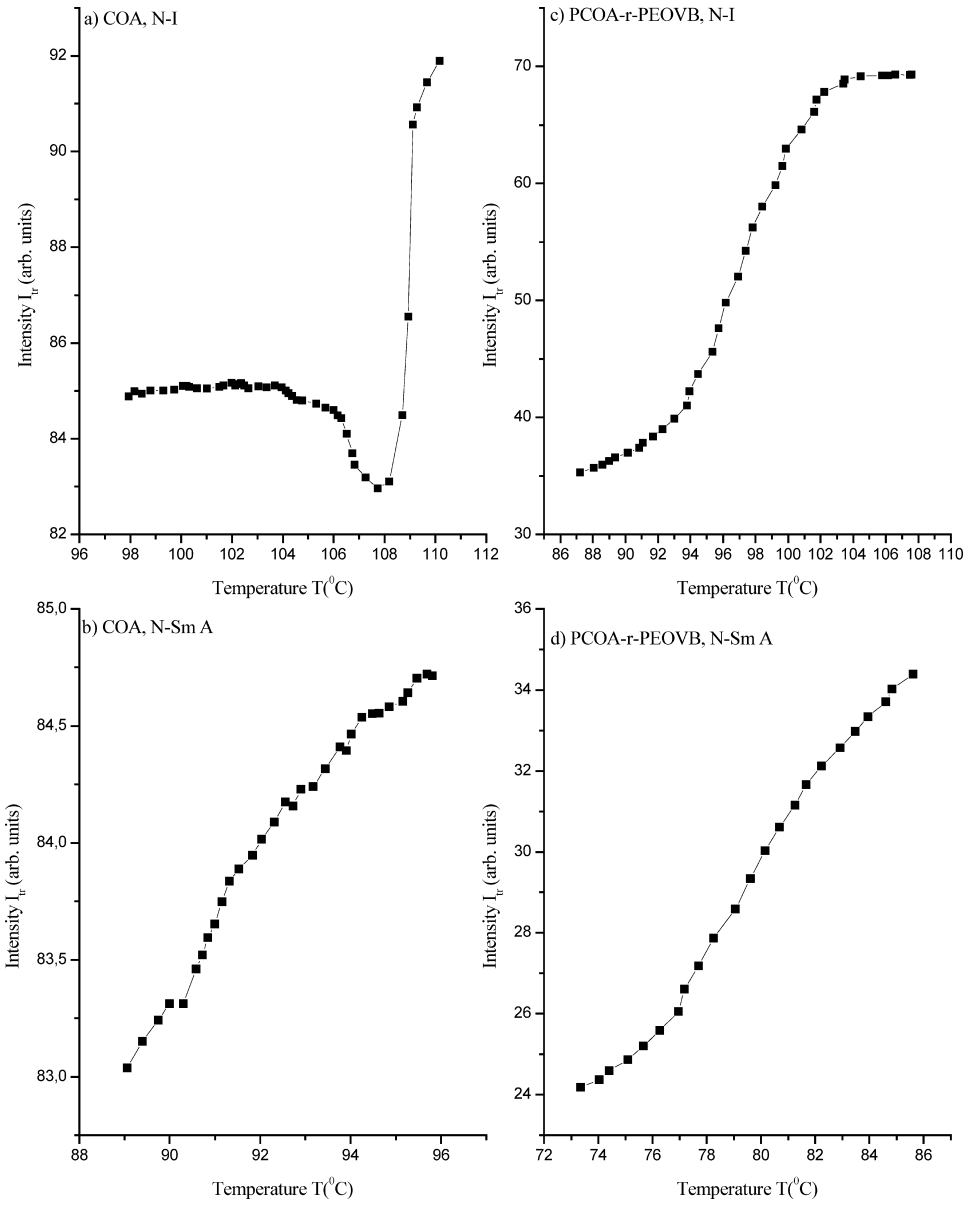

Figure 3. The transmitted light intensity I_{tr} vs. temperature T for COA **(a, b)** and PCOA-*r*-PEOVB **(c, d)** samples near the N-I and N-Sm A transition regions.

progress has been made, but many aspects of the critical fluctuation effects are not yet well understood and this transition remains one of the most intriguing problems in the critical phenomena of liquid crystals (27). The N-Sm A transition is believed to belong to the three-dimensional (3D) XY universality class (28–30). However, the experimental results to date have not established a clear case of 3D XY universality class. The experimental effective critical exponents vary systematically with the range of the nematic phase (28, 31–33). Besides, it has been shown that the N-Sm A transition may be first

or second order with a tricritical point (TCP) separating these two different behaviors. For sufficiently narrow nematic ranges, the transition is of first order (31, 32, 34) becoming second order via a tricritical point for wider nematic ranges (28, 33). Although the Mc Millan ratio $M = T_{NA}/T_{NI}$ where T_{NA} and T_{NI} are the N-Sm A and N-I transition temperatures, respectively, is a measure of the proximity of the N-Sm A transition to the N-I transition (35), namely the width of the nematic range, its value is not universal for different systems. Tricritical points in previously studied systems are characterized by McMillan ratios of 0.942 to 0.995 (18, 23, 31, 36–39), and systems with smaller ratios usually exhibit second order N-Sm A transitions (28).

As seen in Figure 3 (b) and (d), the transmitted intensity I_{tr} decreased drastically at certain temperature intervals corresponding to the N-Sm A transitions of the samples under investigation upon cooling and vice versa upon heating. It is worthwhile pointing out that the difference in the transmitted intensities of the N and Sm A phases arises since the director fluctuations make the former turbid. In smectics, twist and bend are expelled by the presence of a nonzero layer-compression modulus B, hence, smectics are less turbid than nematics. In effect, the transmitted intensiy measured is that of layer-compression modulus B. De Gennes has shown that B is proportional to the square of the magnitude of the smectic order parameter Ψ (26). Since $B \approx |\Psi|^2$, near the N-Sm A transition region, the transmitted intensity we measured in this work is proportional to $|\Psi|^2$. Using this assumption, the intensity I_{tr} can be written as a power law near the critical temperature T_c of the phase transition

$$|I_{tr} - I_{tr_c}| = At^{2\beta} \tag{1}$$

where I_{tr_c} is the value of I_{tr} at T_c, A is the critical amplitude, t is the reduced temperature, $t = 1 - T/T_c$, and β is the critical exponent. We have tried to extract the effective critical exponents at the N-Sm A transition from our I_{tr} vs. T data for the investigated samples. The effective critical exponents have been produced by fitting the data to the double logarithmic form of Eq. (1). During these fits $T_c = T_{NA}$ has been fixed at the value obtained from the extrama of the first derivative of the I_{tr} vs T data. Note that only data 8–9 K below the N-Sm A transition have been considered during the fitting procedure to avoid the fluctuation effects of the successive phases. The normalized I_{tr} vs. T data over the N-Sm A transition region for both COA and PCOA-*r*-PEOVB samples is shown in Figure 4 on a log-log scale. In Table 3, we present the N-Sm A transition temperatures, the effective critical exponents, and the reduced temperature ranges, over which the effective exponents are calculated for COA and PCOA-*r*-PEOVB samples.

It is evident from Table 3 that the N-Sm A transition is continuous but is away from 3D XY universality. Indeed, the effective critical exponents are close to mean-field values (0.5). The nematic ranges are 19.07 K and 18.28 K for COA and PCOA-r-PEOVB samples, respectively. It might be concluded that although the observed nematic ranges are wide enough to drive the N-Sm A transition second order, the critical regions at the N-Sm A transition for our samples are not wide enough to obtain 3D XY exponents as the Ginzburg criterion predicts (40). In our previous work, (41), we investigated the phase transitions of COA monomer, its homopoylmer PCOA, and its graft copolymer with polytetrahydrofuran grafts. The transition temperatures of COA monomer measured in Reference (41) were 3 K less than those measured in the present work since the previous temperature scanning rates were higher than the ones for the present work. At these scanning rates, the probability of the conversion of LC monomer to polymer during the thermal treatment should also be considered. Furthermore, in the

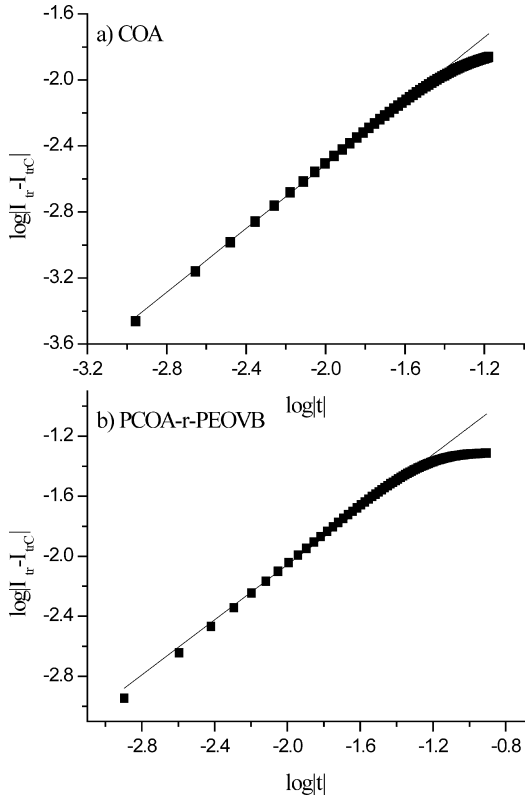

Figure 4. The normalized transmitted intensity vs. $|t|$ over the N-Sm A transition region on log-log scale for **(a)** COA monomer, and **(b)** random-copolymer PCOA-*r*-PEOVB. The solid lines represent the double logarithmic fits to Eq. (1).

previous paper, it was observed that both PCOA homopolymer and its graft copolymer exhibited a N-Sm A transition, that however was of first-order for the former and of second order for the latter, similar to PCOA-*r*-PEOVB for the present work, with the transition temperature remaining the same. It is known that, on general theoretical grounds, first-order phase transitions are converted to second-order phase transitions, by the introduction of frozen disorder into a system (42–44). In the current case, in going

Table 3

The transition temperatures and the effective critical exponents at the N-Sm A transition region for the investigated samples, $t = 1 - T/T_{NA}$, $|t|_{\max}$: upper limit of the fit [refer to Eq. (1)]

Samples	T_{NA} (°C)[a]	β	$\lvert t\rvert_{\max}$	$M = T_{NA}/T_{NI}$
COA	90.51	0.483 ∓ 0.003	0.036	0.95
PCOA-r-PEOVB	78.86	0.459 ∓ 0.005	0.06	0.95

[a]Transition temperatures obtained from *in-situ* measurement (see text), held constant at the indicated values during the fitting procedures.

from PCOA to PCOA-*r*-PEOVB during the synthesis stage, a frozen randomness, in the form of random connectivities is introduced. A similar effect was observed for the graft copolymer of COA with polytetrahydrofuran grafts in the previous work (41). Note that the effective exponent near the N-Sm A transition was close to a mean-field regime for graft copolymer of COA in Reference 41, similar to the PCOA-*r*-PEOVB sample in the current work. It might be concluded that the smallness of the critical region for the N-Sm A transition should be due to the COA monomer.

In the present work, we have also tried to extract the effective exponent at the Sm A-Sm C transition of COA liquid-crystalline monomer. To achieve this, we have used the assumption given above for the Sm C order parameter, namely tilt angle. The transmitted intensity decreased dramatically at the Sm A-Sm C transition for COA sample upon cooling (not shown), similar to that at the N-Sm A transition region. Since the molecules of liquid crystal samples order on passing through the various liquid crystalline phases on cooling, the intensity I_{tr} decreased. Hence, using the assumption that I_{tr} intensity is proportional to the square of the order parameter near the Sm A-Sm C transition, we have produced the effective exponents by fitting the data to double logarithmic form of Eq. (1). For this fit, $T_c = T_{AC}$ has been fixed at the value obtained from *in situ* measurements. Over the reduced temperature range $1.3 \times 10^{-3} < |1 - T/T_{AC}| < 4.04 \times 10^{-2}$ the effective critical exponent was found to be $\beta = 0.5117 \mp 0.0007$ which is consistent with a mean-field Landau model with anomalously large sixth-order term, describing the Sm A-Sm C transition very well (27, 33, 45–48). Note that similar results were found in our previous work (41) at the Sm A-Sm C transition for the COA sample. In that work, β was found to be 0.533 ∓ 0.001 over the reduced temperature

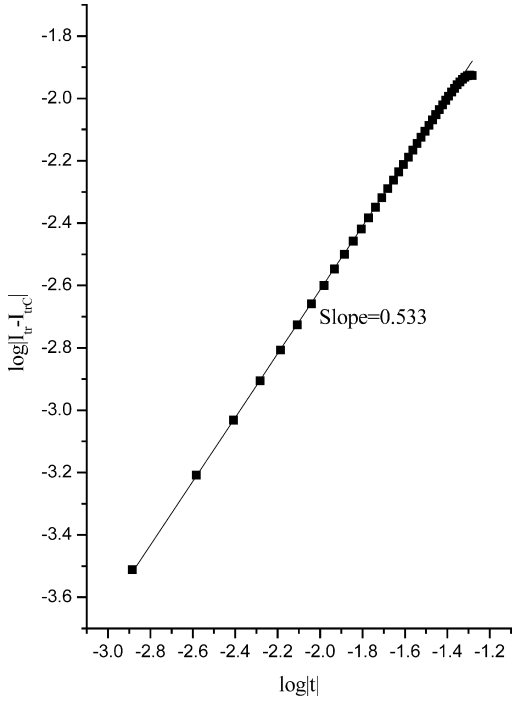

Figure 5. Double logarithmic plot for the normalized intensity vs. $|t|$ at the Sm A-Sm C transition of COA monomer. The solid line is the double logarithmic fit to Eq. (1).

range, which was narrower than the one in the present work. The double logarithmic plot of the normalized intensity vs. reduced temperature near the Sm A-Sm C transition for COA is presented in Figure 5.

It is known that in experiments, hysteresis is always indicative of a first-order phase transition. Thermal hysteresis phenomenon has been studied initially by Rao and Pandit in the framework of O(N)-symmetric $(\Phi^2)^3$ model (49). They obtained a scaling law of the areas of the thermal hysteresis loops with the amplitude and frequency of the periodically oscillating temperature field. It should be noted that, experimentally, a more easily attainable way of varying temperature is by changing it linearly, rather than periodically. Fan and Jinxiu (50) obtained the thermal hysteresis loops under linearly varying temperature based on the O(N)-symmetric $(\Phi^2)^3$ model. They have shown that the areas A of the hysteresis loops can obey the scaling form given by

$$A = A_0 + A_1 R^n \tag{2}$$

where R is the temperature scanning rate, n is the scaling exponent, and A_0 and A_1 are constants. The exponent n approaches two thirds being universal for both the mean-field and field-theoretical models. As mentioned above, the transmitted intensity I_{tr} for the PCOA-*r*-PEOVB sample exhibits a quite large hysteretic behavior near the N-I transition i.e., the phase transition during heating and cooling runs follows different paths. To quantify this behavior, the thermal hysteresis loops were obtained from the I_{tr} vs. T data upon heating and cooling during the N-I and I-N transitions for the random copolymer sample. The temperature was driven linearly with prescribed rates $R = 0.047,\ 0.055,\ 0.067,\ 0.085,$ and $0.105\,\mathrm{K/s}$, and I_{tr} vs. T measurements were repeated to produce the hysteresis loops at different R values. Figure 6 displays a

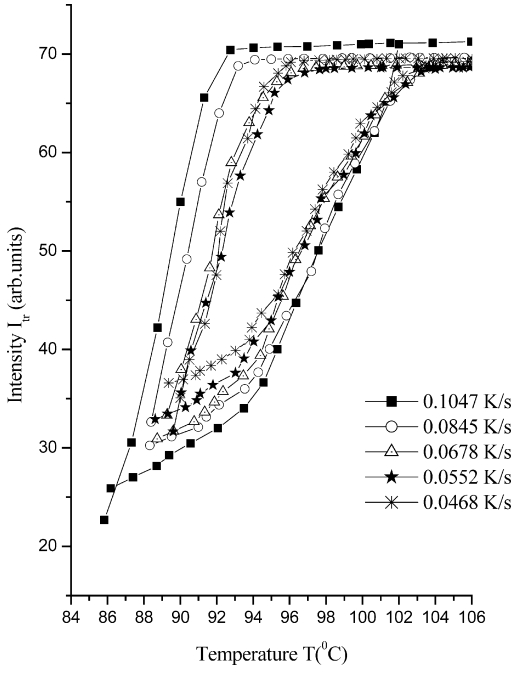

Figure 6. The thermal hysteresis loops at various scan rates R for PCOA-*r*-PEOVB copolymer.

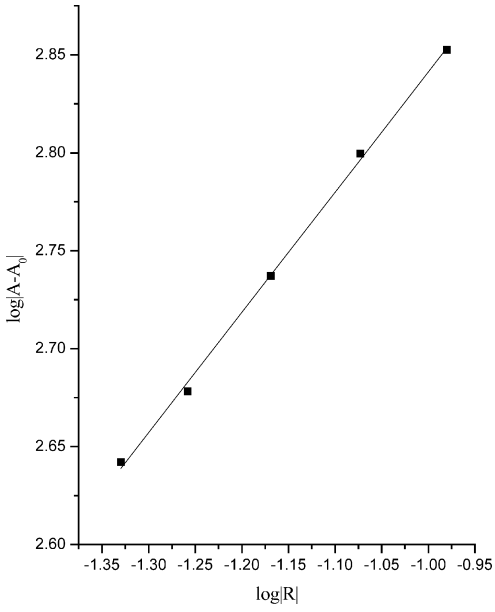

Figure 7. The area A vs. temperature scan rate R on log-log scale. Note that the constant term A_0 has been substracted to give the straight line.

family of R-dependent hysteresis loops for PCOA-*r*-PEOVB sample. The areas A of the hysteresis loops for different scan rates were produced and then the data were fitted to the scaling form given in Eq. (2). The scaling behavior of the areas for the random copolymer on a log-log scale is shown in Figure 7. The scaling exponent n was found to be 0.614 ∓ 0.02 which is less than, but quite close to, the value given by Fan and Jinxiu. Similar scaling behavior of the thermal hysteresis loops for N-I and first-order N-Sm A transitions has been reported previously by our group (23, 51).

Conclusions

PEO macromonomer possessing a *p*-vinylbenzyl end-functional group (PEOVB) was synthesized by living anionic polymerization and employed in free-radical copolymerization with a liquid crystalline monomer, COA. The phase transitions of COA and its random copolymer with PEOVB have been reported. Multiple phase transitions of COA monomer are reduced in random copolymer, and nematic and smectic A phases appear dominant. We have produced the effective exponents for both samples at the N-Sm A transition. It was found that, although the nematic range is wide enough to drive the transition second order, the critical regions of both samples do not allow obtaining 3D XY values. We have also reported the scaling behavior of the thermal hysteresis during the N-I and I-N transitions for PCOA-*r*-PEOVB sample. The hysteresis loops were obtained in the frame of I_{tr} vs T under linearly varying temperature and the scaling exponent n was found to be 0.614 which is in good agreement with the $(\Phi^2)^3$ model value. The thermal hysteresis loops for COA monomer were not as wide as for the random copolymer, thus, we could not obtain a similar scaling behavior for this monomer.

Acknowledgements

O. P. and Y. Y. thank the Academy of Sciences of Turkey (TUBA) for partial support.

References

1. Mishra, M.K. (1994) *Macromolecular Design: Concept and Practice*; New York: Polym. Frontiers Int. Inc., Part 1.
2. Yagci, Y., Nuyken, O., and Graubner, V. (2005) Telechelic Polymers, in Encyclopedia of Polymer Science and Technology, 3rd ed., Kroschwitz, J.I., ed.; New York: Wiley, Vol. 12, 57–130.
3. Mecerreyes, D., Pomposo, J.A., Bengoetxea, M., and Grande, H. (2000) Novel Pyrrole End-Functional Macromonomers Prepared by Ring-Opening and Atom-Transfer Radical Polymerizations. *Macromolecules*, 33: 5846–5849.
4. Matyjaszewski, K., Beers, K.L., Kern, A., and Gaynor, S.G. (1998) Hydrogels by Atom Transfer Radical Polymerization. I. Poly(*N*-vinylpyrrolidinone-*g*-styrene) via the Macromonomer Method. *J. Polym. Sci., Part A: Polym. Chem.*, 36: 823–830.
5. Zeng, F., Shen, Y., Zhu, S., and Pelton, R. (2000) Synthesis and Characterization of Comb-Branched Polyelectrolytes. 1. Preparation of Cationic Macromonomer of 2-(Dimethylamino)ethyl Methacrylate by Atom Transfer Radical Polymerization. *Macromolecules*, 33: 1628–1635.
6. Shen, Y., Zhu, S., Zeng, F., and Pelton, R. (2000) Versatile Initiators for Macromonomer Syntheses of Acrylates, Methacrylates, and Styrene by Atom Transfer Radical Polymerization. *Macromolecules*, 33: 5399–5404.
7. Chiefari, J., Jeffrey, J., Mayadunne, R.T.A., Moad, G., Rizzardo, E., and Thang, S.H. (2000) Preparation of Macromonomers via Chain Transfer with and without Added Chain Transfer Agent. *ACS Symp. Ser.*, 768: 297–312.
8. Ito, K., Tomi, Y., and Kawaguchi, S. (1992) Poly(ethylene oxide) Macromonomers. 10. Characterization and Solution Properties of the Regular Comb Polymers with Polystyrene Main Chains and Poly(ethylene oxide) Side Chains. *Macromolecules.*, 25: 1534–1538.
9. Yilmaz, F., Cianga, I., Ito, K., Senyo, T., and Yagci, Y. (2003) Synthesis and Characterization of α-ε Heterofunctional Poly(ethylene oxide) Macromonomers. *Macromol. Rapid Commun.*, 24: 316–319.
10. Yamamoto, Y., Nakao, W., Atago, Y., Ito, K., and Yagci, Y. (2003) A Novel Macroinimer of Polyethylene Oxide: Synthesis of Hyper-Branched Networks by Photoinduced H-abstraction Process. *Eur. Polym. J.*, 99: 545–550.
11. Yildiz, H.B., Kiralp, S., Toppare, L., Yilmaz, F., Yagci, Y., Ito, K., and Senyo, T. (2005) Conducting Copolymers of 3-Methylthienyl Methacrylate and p-Vinylbenzyloxy Poly(ethyleneoxide) and Their Electrochromic Properties. *Polym. Bull.*, 53: 193–201.
12. Galli, G. (2001) *Advanced Functional Molecules and Polymers*; edited by Nalwa, H.S., ed.; Overseas Publishers Association: Singapore; Vol. 1, 271.
13. Serhatli, I.E., Hepuzer, Y., Yagci, Y., Chiellini, E., Rosati, A., and Galli, G. (2000) Design, Synthesis and Thermal Behavior of Liquid Crystalline Block Copolymers by Using Transformation Reactions. In *Tailored Polymers & Application*; edited by Yagci, Y., Mishra, M.K., Nuyken, O., Ito, K. and Wnek, G., eds.; VSP: Utrecht, 175–197.
14. Yilmaz, F., Kasapoglu, F., Hepuzer, Y., Yagci, Y., Toppare, L., Fernandes, E.G., and Galli, G. (2005) Synthesis and Mesophase Properties of Block and Random Co-polymers of Electroactive and Liquid Crystalline Monomers. *Des. Monomers Polym.*, 8: 223–236.
15. Demus, D., Goodby, J., Gray, G.W., Spiess, H.W., and Vill, V. (1998) *Handbook of Liquid Crystals*; Wiley-VCH: Wienheim; Vol. 3.
16. Ozbek, H., Yildiz, S., and Pekcan, O. (1999) Photon Transmission Technique for Studying Multiple Phase Transitions in a Liquid Crystal. *Phys. Rev.*, E59: 6798.

17. Ozbek, H., Yildiz, S., Pekcan, O., Hepuzer, Y., Yagci, Y., and Galli, G. (2002) Study of Phase Transitions in Liquid Crystalline Side Group Polymers via Photon Transmission Method. *Mater. Chem. Phys.*, 78: 318–322.
18. Yildiz, S., Serhatli, I.E., Pekcan, O., Berker, A.N., and Ozbek, H. (2002) A Phase Diagram of Smectogen-non-Smectogen Binary Mixture: A Photom Transmission Study. *Int. J Mod. Phys.*, B16: 3959–3970.
19. Özbek, H. and Pekcan, Ö (2004) Critical exponents of Thermal Phase Transitions in Kappa-carrageenan-water System. *J. Mol. Struct. Theochem.*, 676: 19–27.
20. Shen, R., Senyo, T., Akiyama, C., Atago, Y., and Ito, K. (2003) One-step Synthesis of α-*p*-Vinylphenylalkyl-ω-hydroxy Poly(ethylene oxide) Macromonomers by Anionic Polymerization I.nitiated from *p*-vinylphenylalkanols. *Polymer*, 44: 3221–3228.
21. Dubois, J.C., Decobert, G., Le Barny, P., Friedrich, S.C., and Noel, C. (1986) Liquid-Crystalline Side-Chain Polymers Derived from Poly-acrylate, Poly-methyacrylate and Poly-alpha-chloroacrylate. *Mol. Cryst. Liq. Cryst.*, 137: 349–364.
22. De Jeu, W.H. (1980) *Physical Properties of Liquid Crystalline Materials*; Gordon and Breach Science Pub.: New York, Chap. 2.
23. Yildiz, S., Pekcan, O., Berker, A.N., and Ozbek, H. (2004) Scaling of Thermal Hysteresis at Nematic-smectic-A Phase Transition in a Binary Mixture. *Phys. Rev.*, E69: 031705.
24. Senyo, T., Atago, Y., Liang, H., Shen, R., and Ito, K. (2003) Syntheses of Poly(ethylene oxide) Macromonomers Carrying Tertiary Amine And Quaternary Ammonium End Group. *Polym. J.*, 35: 513–518.
25. Maier, V.W. and Saupe, A. (1958) Eine Einfache Molekulare Rheorie Des Nemotischen Kristaleinflussigen Zustandes. *Z. Naturforsh.*, 13 (7): 564–566, (1959) Eine einfache molekularstatistische Theorie der Nematischen Kristallinflüssigen Phase Teil I, *Z. Naturforsh.* 14a: 882–889.
26. De Gennes, P.G. and Prost, J. (1993) The Physics of Liquid Crystals. Clarendon Press: Oxford.
27. Thoen, J. (1995) Thermal Investigations of Phase-transitions in Thermotropic Liquid-Crystals. *Int. Mod. Phys.*, B9: 2157–2218 (and references cited therein).
28. Garland, C.W. and Nounesis, G. (1994) Critical-Behavior at Nematic Smectic-A Phase-Transitions. *Phys. Rev.*, E49: 2964–2971 (and references cited therein).
29. (a) Halperin, B.I., Lubensky, T.C., and Ma, S.K.. First-order Phase-transitions in Superconductors and Smectic-A Liquid-Crystals. *Phys. Rev. Lett.*, 1974, 32: 292–295; (b) Dasgupta, C., Halperin, B.I. (1981) Phase-transition in a Lattice Model of Superconductivity. *ibid.*, 47: 1556–1560; (c) Lubensky, T.C. (1983) The Nematic to Smectic-A Transition—A Theoretical Overview. *Journal De Chimie Physique Et De Physico-Chimie Biologique.*, 80 (1): 31–43.
30. Patton, B.R. and Andereck, B.S. (1992) Extended Isotropic-to-Anisotropic Crossover above the Nematic Smectic-A Phase-Transition. *Phys. Rev. Lett.*, 69: 1556–1559.
31. Thoen, J., Marynissen, H., and Van Dael, W. (1984) Nematic-Smectic-A Tricritical Point in Alkylcyanobiphenyl Liquid-Crystals. *Phys. Rev. Lett.*, 52: 204–207.
32. Ocko, B.M., Birgeneau, R.J., and Litster, J.D. (1986) Crossover to Tricritical Behavior at the Nematic to Smectic-A Transition-an X-Ray-Scattering Study. *Z. Phys.*, B62: 487–497.
33. Thoen, J. (1992) *Phase Transitions in Liquid Crystals*; Martellucci, S. and Chester, A.N., eds.; Plenum Press: New York, Chap. 10, p.155; Garland, C.W. ibid, Chap. 11, p. 175 and references cited therein.
34. Marynissen, H., Thoen, J., and Van Dael, W. (1985) Experimental-Evidence for a Nematic to Smectic-a Tricritical Point in Alkylcyanobiphenyl Mixtures. *Mol. Cryst. Liq. Cryst.*, 124: 195–203.
35. Mc Millan, W.L. (1971) Simple Molecular Model for the Smectic *A* Phase of Liquid Crystals. *Phys. Rev.*, A4: 1238–1246.
36. Brisbin, D., De Hoff, R.J., Lockhort, T.E., and Johnson, D.L. (1979) Specific Heat near the Nematic-Smectic-*A* Tricritical Point. *Phys. Rev. Lett.*, 43: 1171–1174.
37. Stine, K.J. and Garland, C.W. (1989) Calorimetric Study of Nematic to Smectic-A Tricritical Behavior. *Phys. Rev.*, A39: 3148–3156.

38. Anisimov, M.A., Voronov, V.P., Kolkov, A.O., Petuklov, V.N., and Kholmurodov, F. (1987) High-Resolution Adiabatic Calorimetry Measurements in the Vicinity of the Liquid-Crystal Phase-Transitions. *Mol. Cryst. Liq. Cryst.*, 150: 399–418.
39. Nounesis, G., Garland, C.W., and Shashidhar, R. (1991) Crossover from Three-Dimensional XY to Tricritical Behavior for the Nematic–Smectic-A_1 Phase Transition. *Phys. Rev.*, A43: 1849.
40. Ginzburg, V.L. (1961) Some Remarks on Phase Transitions of The 2nd Kind And The Microscopic Theory of Ferroelectric Materials, Sov. *Phys. Solid State.*, 2 (9): 1824–1834.
41. Ozbek, H., Yildiz, S., Pekcan, O., Hepuzer, Y., Yagci, Y., Berker, A.N., Galli, G., and Chiellini, E. (2003) Comparative Study of Liquid Crystalline Ordering in a Monomer, Linear Polymer and Graft Copolymer via the Photon Transmission Technique. *Phase Transit.*, 76: 991–998.
42. Hui, K. and Berker, A.N. (1989) Random-field Mechanism in Random-bond Multicritical Systems. *Phys. Rev. Lett.*, 62: 2507–2510.
43. Berker, A.N. (1991) Absence of Temperature-Driven First-Order Phase Transitions in Systems with Random Bonds (invited). *J Appl. Phys.*, 70: 5941–5945.
44. Berker, A.N. (1993) Critical Behavior Induced by Quenched Disorder. *Physica A.*, 194: 72–76.
45. Huang, C.C. and Viner, J.M. (1982) Nature of the Smectic-*A*—Smectic-*C* Phase Transition in Liquid Crystals. *Phys. Rev.*, A25: 3385–3388.
46. Birgeneau, R.J., Garland, C.W., Kortan, A.R., Litster, J.D., Meichle, M., Ocko, B.M., Rosenblatt, C., Yu, L.J., and Goodby, J. (1983) Smectic-*A*-smectic-*C* Transition: Mean Field or Critical. *Phys. Rev.*, A27: 1251–1254.
47. Thoen, J. and Seynaeve, G. (1985) Calorimetric Investigations of the Liquid-Crystalline Material Heptyloxybenzylidene-Heptylaniline (70.7). *Mol. Cryst. Liq. Cryst.*, 127: 229–256.
48. Huang, C.C. (1987) *Theory and Applications of Liquid Crystals*; Ericksen, J.L. and Kinderlehrer, D., eds.; Springer-Verlag: New York(and references cited therein).
49. Rao, M. and Pandit, R. (1991) Magnetic and Thermal Hysteresis in the $O(N)$-symmetric $(\Phi^2)^3$ model. *Phys. Rev.*, B43: 3373–3386.
50. Fan, Z. and Jinxiu, Z. (1995) Scaling of Thermal Hysteresis with Temperature Scanning Rate. *Phys. Rev.*, E51: 2898–2901.
51. Yildiz, S., Zayim, E.O., Pekcan, O., and Ozbek, H. Unpublished results.